Study on Microwave Remote Sensing of Atmosphere, Cloud and Rain①

Zhao Bolin (赵柏林)
Department of Geophysics, Peking University, Beijing 100871
Received November 27, 1989

ABSTRACT

In this paper, recent research of microwave remote sensing of atmosphere, cloud and rain in China is presented. It includes the following aspects:

(1) Progress in the development of multifrequency radiometer and its characteristics and parameters;

(2) Application of microwave remote sensing in prediction of atmospheric boundary layer. The atmospheric temperature profiles are derived with 5 mm (54.5 GHz) radiometer angle-scanning observations. Due to the fact that microwave radiometer could monitor the atmospheric temperature profile continuously and make the initialization of numerical model any time, it is helpful for improving the accuracy in prediction of the evolution of atmospheric boundary layer;

(3) Theory and application of microwave radiometers in monitoring atmospheric temperature, humidity and water content in cloud. The field experiment of International Satellite Cloud Climatology Project (ISCCP) at Shionomisaki and Amami Oshima of Japan for studies of cloud and weather has been described;

(4) Satellite remote sensing of atmosphere and colud. The TIROS-N TOVS satellite data are used to obtain atmospheric temperature profile. The results are compared with those of radiosonde, with rms deviation smaller than that of the current operational TOVS processing;

(5) Microwave remote sensing and communication. The atmospheric attenuations are derived with microwave remote sensing methods such as solar radiation method etc., in order to obtain the local value instantaneously. The characteristics of Beijing's rainfall have been analysed and the probability of microwave attenuation of rain is predicted;

(6) For improvement of the accuracy of rainfall measurement, a radiometer-radar system ($\lambda = 3.2$ cm) has been developed. The variation of rainfall distribution and area-rainfall may be obtained by its measurements, which may be helpful for hydrological prediction.

The prospect of microwave remote sensing in meteorology is also discussed.

I. INTRODUCTION

The microwave remote sensing of atmosphere is an important subject in the atmospheric sciences. It gives us new atmospheric information, with which monitoring of atmospheric properties and prediction of weather processes may be improved. In the last 20 years, research on microwave remote sensing of atmosphere has been carried on in China. In this paper, some recent research results obtained in China are discussed.

Derivation of the atmospheric property from remotely sensed microwave radiation is a

---

①Special Announcement: Starting with Volume 8, 1991, Advances in Atmospheric Sciences will be both published and distributed worldwide by China Ocean Press. For subscription information please contact us directly (see subscription sheet for details).

hopeful method of atmospheric exploration. By means of reception of atmospheric emission, we can make remote sensing of atmospheric temperature–humidity profile, obtain the parameters of cloud and rain, and monitor the weather process. Owing to its mobile, flexible, quick and continuous sampling characteristics, ground–based microwave remote sensing would be helpful for nowcasting, pollution meteorology, artificial precipitation, etc. On the other hand, satellite microwave remote sensing is a hopeful method for measurements of atmosphere, cloud and rain.

Described in this paper are some recent research results such as progress in development of multifrequency radiometer; microwave remote sensing to improve the prediction of the atmospheric boundary layer; microwave remote sensing of atmosphere, cloud and rain, including experimental results of North–Western Pacific Cloud Radiation Experiment of International Satellite Cloud Climatology Project (ISCCP); retrieval of TIROS–N TOVS to derive the atmospheric temperature profile; measurements of atmospheric attenuation with microwave remote sensing method in order to obtain the local and instantaneous value; analyses of the rainfall of Beijing for predicting the rain attenuation in the surface–satellite link communication; the structure of radiometer–radar system and its measurement of areal rainfall in reservoir district. Finally, prospects of remote sensing in meteorology are also discussed.

II. PROGRESS IN DEVELOPMENT OF MULTIFREQUENCY MICROWAVE RADIOMETER

Peking University in cooperation with the Dahua Radio Factory has constructed a 5 mm–1.35 cm microwave radiometer system. It is of compensative Dicke's type. We have renewed the system through 5 generations and then put it into practice. The waveband 5 mm (frequencies 52.9 and 54.5 GHz) is used to measure atmospheric temperature profile, 1.35 cm (frequency 22.235 GHz) for atmospheric humidity, 8 mm (frequency 35.3 GHz) for cloud water content and 3.2 cm (frequency 9.37 GHz) for rain (see Zhao et al., 1981; 1985 a, b, c; 1987; Zhao, 1987; 1988).

Threshold antenna temperature ΔT_A is a parameter of radiometer sensitivity, and can be written as

$$\Delta T_A = \frac{\alpha^* (T_R + T_A)}{\sqrt{B\tau}} \tag{1}$$

where T_A and T_R are antenna temperature and radiometer noise temperature, respectively; B bandwidth, τ integral time, and $\alpha^* = 2$.

Take ΔT_A (τ = 1sec) as a standard scale for comparison with each other, as shown in Fig.1. The sensitivity of the microwave radiometer system of Peking University in 1981 was at the same level as the average level of radiometers in the world, However, since 1985 it has been better than the average level and come into the advanced ranks (see Handbook, 1987; Hoggs et al., 1983; Nimbus–5, 1972; Nimbus–6, 1974).

For the past few years, the 3 cm, 8 mm and 1.35 cm radiometers have been developed by the Institute of Atmospheric Physics, Academia Sinica for meteorological aim (see Zhao et al., 1983; Zhou et al., 1982; Huang and Zou, 1987).

Nowadays the progress of microwave radiometers is toward combining multifrequency radiometer into one united set in order to improve the resolution, and toward automatic observation and data processing. In the following, the 8 mm–1.35 cm dual–channel radiometer, made in Peking University (1988), will be described. Its structure is shown in Fig.2.

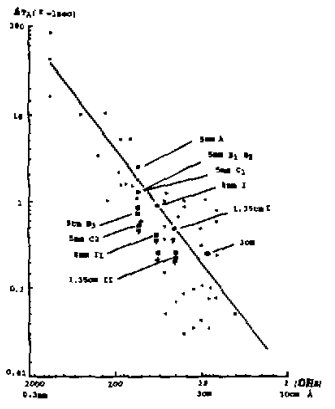

Fig.1. The sensitivity of microwave radiometers. · International level of microwave radiometer (Handbook of remote sensing techniques, 1973); + Nimbus – 6 SCAMS; ∇ Nimbus – 5 NEMS; ⊙ NOAA – Lab wave propagation, profiler; o microwave radiometers of ours (1981); * microwave radiometers of ours (1985).

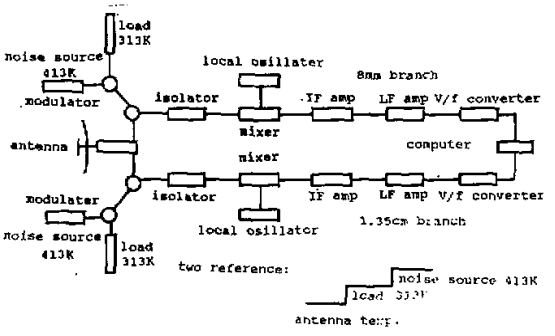

Fig.2. Structure of the 8 mm – 1.35 cm dual–channel microwave radiometer.

The radiometer has an antenna for 8 mm–1.35 cm waveband. Signals enter a circular waveguide feed and are separated by waveguide polarization with different frequencies, then go into 8 mm and 1.35 cm receivers independently. They are two reference loads with temperatures of 313 K and 413 K. They are put into each receiver, and used to calibrate the receiver's gain. Signals pass through mixer and amplifiers and then output to Apple–II computer for sampling and data processing. With antenna zenith observations, the profile of atmospheric water vapor content may be derived. Microwave radiometer observations can be carried on with elevation and azimuthal angle scanning, then the distribution of cloud water content of whole sky is obtained. The data processing and radiometer observations are automatically conducted by use of an Apple–II microcomputer.

III. APPLICATION OF MICROWAVE REMOTE SENSING IN PREDICTION OF THE ATMOSPHERIC BOUNDARY LAYER

In this paper, a method of 5 mm (54.5 GHz) radiometer observations combining with the numerical model for atmospheric boundary layer prediction is presented. The atmospheric temperature profile, derived by 5 mm (54.5 GHz) radiometer, could monitor the atmospheric stratification continuously, and could make the initialization of numerical model any time, so that it provides assistance for improving the accuracy in prediction of the evolution of atmospheric boundary layer.

1. *Improving the Accuracy in* 5 mm (54.5 GHz) *Microwave Radiometer Lower Atmospheric Temperature Profile Measurements*

Ground–based observations of 5 mm oxygen absorption band have been used to get atmospheric temperature profile. A 5 mm (54.5 GHz) radiometer is employed to make elevation angle scanning observations. In this band, there exists a small value of water vapor absorption. On the ground, the brightness temperature of received atmospheric noise, $T_B(v,\ \theta)$, can be written as

$$T_B(v,\ \theta) = T_\infty e^{-\int_0^\infty \alpha\sec\theta dz} + \int_0^\infty T(z)\alpha\sec\theta e^{-\int_0^\infty \alpha\sec\theta dz} dz \ , \tag{2}$$

where v is frequency, θ zenith angle, $T(z)$ temperature, z height, T_∞ cosmic radiation (2.7 K) and α absorption coefficient. With angle–scanning observations, we have a series of brightness temperatures, $T_B(\theta)$. Then by means of Eq.(2), we can inverse the temperature profile $T(z)$. The retrieval method is as follows:

(1) Partially differentiating Eq.(2) with respect to θ , we have

$$\frac{\partial T_B}{\partial\theta} = \int_0^\infty \frac{\partial T}{\partial z} W_1(z)dz = \int_0^\infty \frac{\partial T}{\partial z}\frac{\partial}{\partial\theta} e^{-\int_0^z \alpha\sec\theta dz} dz \ , \tag{3}$$

where $W_1(z) = \dfrac{\partial}{\partial\theta}\exp(-\int_0^z \sec\alpha dz)$. For a certain angle θ, $W_1(z)$ has a maximum value with height, as shown in Fig.3.

(2) From $T_B(v,\ \theta)$, the lst term of right hand of Eq.(2) may be removed, because it is a small value. Combining Eq.(2) of angle θ_1 and θ_2 linearly, we have

$$I(\theta_1,\theta_2) = T_B(v,\theta_1)\cos\theta_1 - T_B(v,\theta_2)\cos\theta_2 = \int_0^\infty T(z)W_2(z)dz$$

$$= \int_0^\infty T(z)\alpha(e^{-\int_0^\infty \alpha\sec\theta_1 dz} - e^{-\int_0^\infty \alpha\sec\theta_2 dz})dz \ , \tag{4}$$

where $W_2(z) = \alpha(e^{-\int_0^z \alpha\sec\theta_1 dz} - e^{-\int_0^z \alpha\sec\theta_2 dz})dz$. For certain θ_1 and θ_2, $W_2(z)$ has a maximum value with height, as shown in Fig.4. From Eqs. (3) and (4), with Chahine relaxation method (1970) the temperature profile and the lapse rate of temperature may be gotten. Let deviation value $R^{(n)}$ have the form

$$R^{(n)} = \frac{\bar{T}(\theta_1,\theta_2) - T^{(n)}(\theta_1,\theta_2)}{\bar{T}(\theta_1,\theta_2)} < \varepsilon \ , \tag{5}$$

where $\bar{T}(\theta_1,\theta_2)$ is the observational value, $T^{(n)}(\theta_1,\theta_2)$ the nth iterative value and $T^{(n)}(z)$ the nth iterative temperature profile.

The results of 5 mm (54.5 GHz) radiometer remote sensing was compared with those of low-level radiosonde. The intercomparison experiments were carried out at Peking University, as shown in Fig.5 where we can see the mean deviation smaller than 1 K (z = 1000 m).

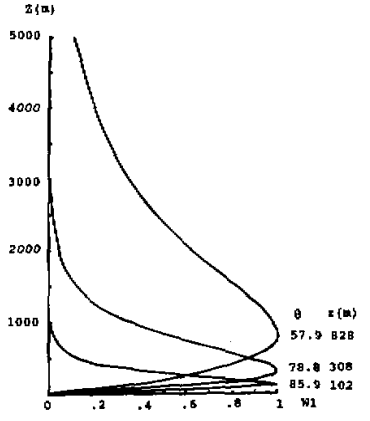

Fig.3. Weighting function W_1 against height z(ν = 54.5 GHz).

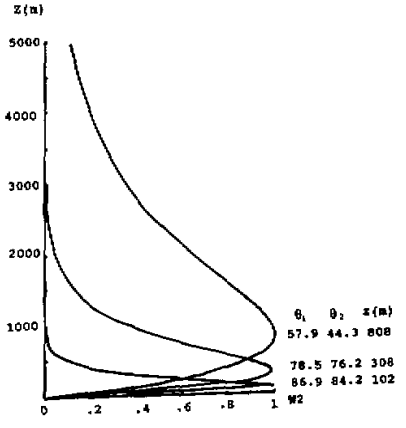

Fig.4. Weighting function W_2 against height z(ν = 54.5 GHz).

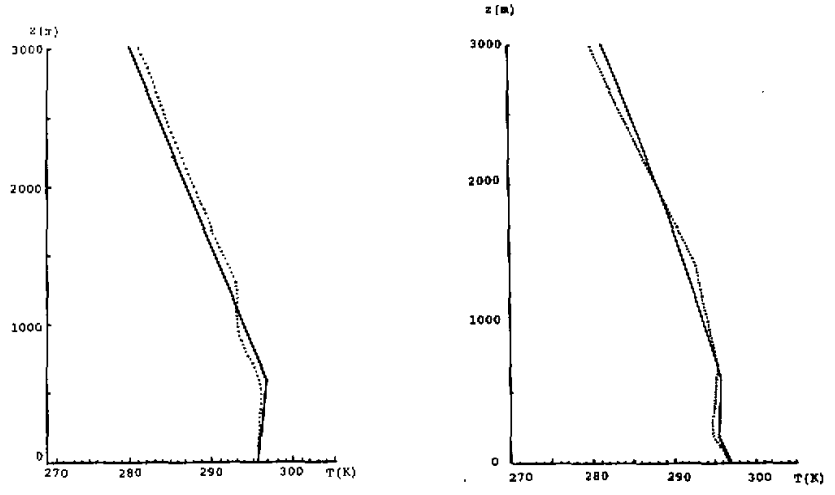

Fig.5. (a) Temperature profile for 07:00 12 July 1986, Beijing. cloud Sc cug (3 / 3). ..... radiosonde; — microwave radiometer ($\nu = 54.5$ GHz).

(b) Temperature profile for 07:00, 21 July 1986, Beijing. cloud Actra Ci dens. ..... radiosonde; — microwave radiometer ($\nu = 54.5$ GHz).

2. *Model and Prediction of Atmospheric Boundary Layer*

The equation of atmospheric boundary layer was solved by Zhang and Anthes (1982) method with the parameterization of diffussion coefficients of Blackadar (1979), the radiation formula of Garratt and Brost (1981), and the axis–transformation of Delage (1974). Owing to that the temperature profile can be monitored continuously, the initialization of numerical model can be made continuously, thus it is helpful for the prediction of the evolution of atmospheric boundary layer. The time intervals of initialization and prediction are 3 hours. Accordingly, 5 mm (54.5 GHz) radiometer remote sensing atmospheric temperature profile promotes the prediction of the evolution of atmospheric boundary layer. Examples are shown in Fig.6 for June 22–23 1985, Peking University, Beijing. The weather was clear and stable. In Fig.6, the prediction of the evolution of atmospheric boundary layer is in agreement with real measurements. Before sunrise there existed a weak inversion, the prediction is as same as the real measurements. They are coincident with each other.

Fig.7 shows the potential temperature distribution of 23 June in daytime in unstable conditions. The evolution of mixing layer may be assessed from the distribution of potential temperature. If we define the height of mixing layer as the height of $\partial\theta^* / \partial z = 0$, then the mixing height of numerical model prediction is coincident with that of resl measurements.

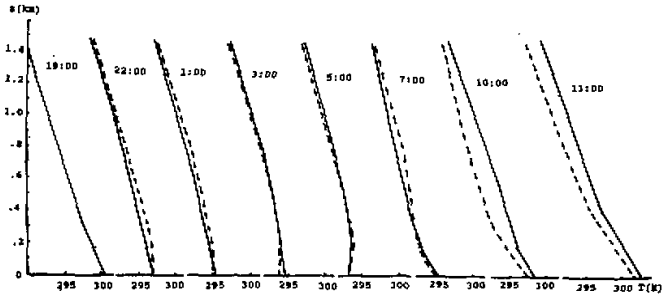

Fig.6. Diurnal variation of temperature profile. Broken lines stand for prediction by numerical model (initialization of temperature profile with microwave remote sensing). Solid lines for measurements by microwave radiometer ($\upsilon = 54.5$ GHz, 22–23 June 1985, Beijing).

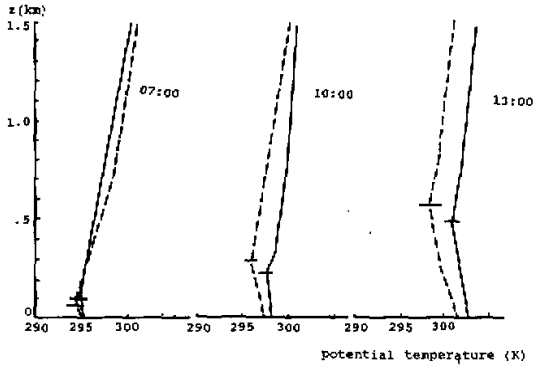

Fig.7. Potential temperature against height. —— model prediction; —, measured with microwave radiometer ($\upsilon = 54.5$ GHz); – height of mixing layer; 23 June 1985, Beijing.

IV. MICROWAVE REMOTE SENSING of CLOUD, RAIN AND WEATHER

In cloudy sky, atmospheric microwave radiation is greatly affected. From atmospheric microwave noises, the cloud parameters may be derived. From remote sensing measurements of 8 mm and 1.35 cm radiometers, the atmospheric water vapor content, liquid water content of cloud and characteristics of absorption in $\lambda = 1.35$ cm water vapor band and $\lambda = 8$ mm window band can be obtained. From the historical radiosonde data in Beijing, a relationship may be found between the absorption of water vapor in $\lambda = 1.35$ cm, $\tau_{H_2O}(22)$ and the absorption of water vapor in $\lambda = 8$ mm, $\tau_{H_2O}(35)$ as

$$\tau_{H_2O}(22) = a\tau_{H_2O}(35) , \tag{6}$$

where $a = 2.8$ for April–June, Beijing.

The absorptions of water vapor $\tau_{H_2O}(22)$ and $\tau_{H_2O}(35)$ are proportional to the water vapor content.

The absorption of cloud α_{Cl} is in proportion to the square of frequency v^2. Between the absorption of cloud in $\lambda = 1.35$ cm $\tau_{Cl}(22)$ and that in $\lambda = 8$ mm. $\tau_{Cl}(35)$ exists a relation

$$\tau_{Cl}(22) = 0.4\tau_{Cl}(35) , \tag{7}$$

i.e., 1.35 cm band brightness temperature depends mainly on atmospheric water vapor content and 8 mm brightness temperature mainly reveals the liquid water content of cloud.

From historical radiosonde data and models with different kinds of clouds by use of Eq.(2), the relationships between the total atmospheric vapor content V, liquid water content of cloud L and brightness temperatures of 1.35 cm and 8 mm, may be derived statistically. For example, in April–June, Beijing, we have for small value of cloud liquid water content (0.02–0.1 mm):

$$V = 0.2412 + 0.05353B_1 - 0.02888B_2 + 1.6228 \times 10^{-4}B_2^2 \tag{8}$$
$$\gamma = 0.99 , \quad s = 0.13\text{cm}$$

$$L = -0.1329 - 5.1946 \times 10^{-3}B_1 + 0.0146B_2 + 3.8928 \times 10^{-5}B_1B_2 \tag{9}$$
$$\gamma = 0.99 , \quad s = 0.025\text{mm}$$

For large value of cloud liquid water content (0.1–4 mm):

$$V = -1.003 + 0.0808B_1 - 0.0216B_2 - 7.027 \times 10^{-5}B_2^2 \tag{10}$$
$$\gamma = 0.98 , \quad s = 0.19\text{cm}$$

$$L = -0.3587 + 0.01233B_2 + 5.6578 \times 10^{-5}B_2^2 \tag{11}$$
$$\gamma = 0.98 , \quad s = 0.23\text{mm}$$

where, B_1 is brightness temperature of $\lambda = 1.35$ cm, B_2 brightness temperature of $\lambda = 8$ mm, γ correlation coefficient, and s rms deviation.

With microwave radiometer observations, the total water vapor content has been obtained, and is compared with that of radiosonde, as shown in Fig.8.

In cloudy case, the brightness temperature of cloudy sky may be corrected to the cloud effect by use of the results of 8 mm and 1.35 cm radiometer observations and the equivalent brightness temperature of clear sky can be obtained. With angle–scanning observations of 5 mm radiometer, and correction of cloud effect by 8 mm and 1.35 cm radiometers, the inversion method with equivalent brightness temperature is as same as that of the clear sky condition (statistical and iterative), and the temperature profile of clear sky may be gotten as shown in Fig.9.

In the North Western Pacific Cloud Radiation Experiment of the International Satellite Climatology Cloud Project (ISCCP), the cloud property has been studied with microwave radiometers. The experimental results in Feb. –Mar. 1989 at Shionomisaki and in Jan. 1990 at Amami Oshima of Japan, are shown as follows: The instruments used are 5 mm microwave radiometer, 8 mm–1.35 cm dual–channel microwave radiometer, 8–13μm infared radiometer,

barometer and Assman psychrometer. With microwave radiometer angle-scanning observations, the temperature profile, the water vapor content, both total and profile, and liquid water content of cloud can be obtained. The results obtained by microwave radiometer were compared with those of radiosonde (at Shionomisaki and Amami Oshima Observatories), with the rms deviation of total water vapor content being 5% and that of temperature below 700 hPa being 1.56 K.

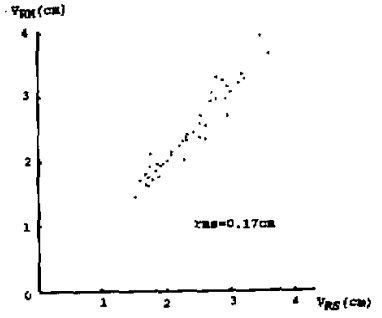

Fig.8. Microwave remote sensing total water vapor content V_{RM} vs radiosonde-measured total water vapor content V_{RS}. All weather (except rain $n=44$), rms = 6.9%.

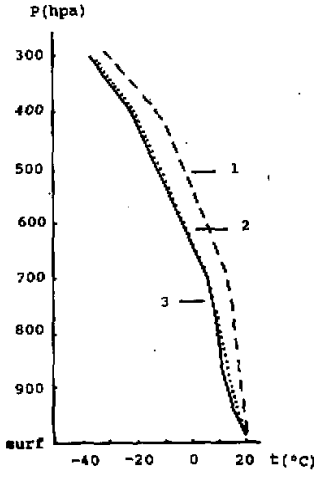

Fig.9. Microwave remote sensing atmospheric temperature profile (07:00 May 30, 1985, Beijing, $v=52.9$ GHz angle scanning observation and statistical retrieval). $L=0.13$ mm, $V=3.16$ cm (by 8 mm and 1.35 cm radiometers' observation); —— remote sensing (without cloud correction); .... remote sensing (with cloud correction); —— radiosonde.

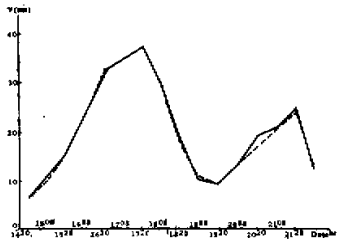

Fig.10. Variation of total water vapor content.

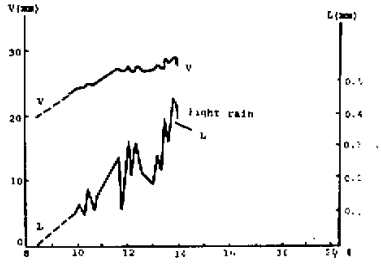

Fig.11. The variations of total water vapor content and liquid water content of cloud before rain begins.

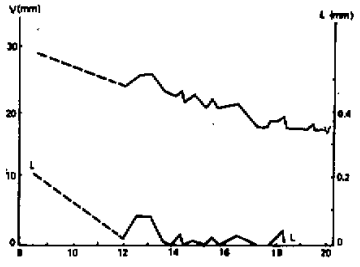

Fig.12. The variation of total water vapor content and liquid water content after rain stops.

Continuous observations of microwave radiometer can be used to monitor the change of air mass as shown in Fig.10. The variation of total water vapor content and liquid water content of colud before and after rains can be obtained by continuous observations (Figs.11 and 12).

A ship–borne dual–wavelength (1.35 cm and 0.85 cm) radiometer of Institute of Atmospheric Physics, Academia Sinica joined the Survey over Tropical Western Pacific Program. From the Survey, the total vapor distribution in clear day over tropical western Pacific Ocean could be found and the result is consistent with average multiannual distribution of water vapor over the Western Pacific Ocean (see Wei et al., 1989).

V. SATELLITE REMOTE SENSING OF ATMOSPHERE AND CLOUD

1. *Remote Sensing of Atmospheric Temperature Profile with Satellite TIROS-N TOVS Data*

The radiative transfer equation of satellite observation is as follows:

$$I_i = \chi_i B(T_s)\tau_i(p_s) - \int_0^{p_s} B_i(T)\frac{\partial \tau_i}{\partial p}dp \ , \tag{12}$$

where I_i is ith channel radiance of satellite observation, χ_i ith channel surface emissivity, B_i Planck constant, T_s surface temperature, p_s surface pressure, and τ_i ith channel atmospheric transmittance.

By formula (13), we have

$$\Delta T_{B_i} = K_{io}\Delta T_s + \sum_{j=1}^{*} K_{ij}\Delta T_j + \sum_{j=1}^{*} K'_{ij}\Delta W_j \ , \tag{13}$$

where ΔT_{B_i} is ith channel brightness temperature difference between observation value and estimate value, ΔW_j jth layer water vapor difference between observation value and estimate value, ΔT_j jth layer temperature difference between observation value and estimate value, and K_{io}, K_{ij}, K'_{ij} are parameters as function of the estimate value. The temperature profile may be retrieved with 4 less-cloud-effect channels and their combination (Table 1). The distribution of weighting function with height is shown in Fig.13. By successive regression method, 5000 pictures of NOAA 9 and NOAA 10 (1986-1988) in 113 orbiting lines have been used to retrieve atmospheric temperature profile. The retrieved results, between 1000 hPa and 10 hPa have the rms deviation of 1.36 K. The accuracy of the above method is higher than that of the current operational TOVS processing.

An example of remote sensing atmospheric temperature profile by ground-based radiometer combining with satellite radiomater observations has been carried out. The result is better than that of ground-based or satellite observations only.

Table 1. Channels of TIROS-N TOVS for Remote Sensing Atmospheric Temperature Profile

channel	central frequency	central wavelength	peak height	absorption gas	aim of exploration
HIRS-1	669cm^{-1}	14.95μm	30hPa	CO_2	temperature
MSU-2	53.74GHz	0.56cm	700hPa	O_2	temperature
MSU-3	54.96GHz	0.55cm	300hPa	O_2	temperature
MSU-4	57.95GHz	0.52cm	90hPa	O_2	temperature
NEW1(MSU2+ 0.5MSU3)			500hPa	O_2	temperature
NEW2(MSU2+ 1.5MSU3)			350hPa	O_2	temperature
NEW3(MSU3+ 0.4MSU4)			150hPa	O_2	temperature

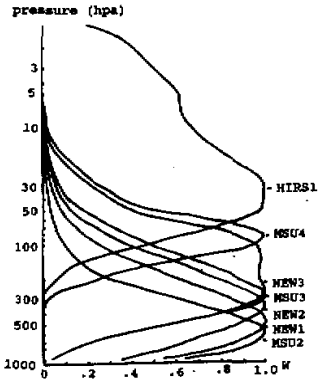

Fig.13. Weighting function. NEW1: (MSU−2)+0.5x(MSU−3) NEW2: (MSU−2) +1.5x(MSU−3); NEW3: (MSU−3)+0.4x(MSU−4).

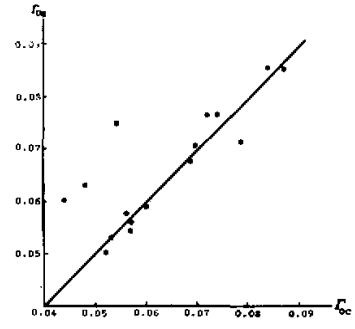

Fig.14. Atmospheric attenuation derived with microwave radiometry (solar method). $\lambda = 8.5$ mm; Γ_{or}: microwave remote sensing; Γ_{oc}: calculated with radiosonde data.

VI. MICROWAVE REMOTE SENSING AND MICROWAVE COMMUNICATION

Microwave attenuation by atmosphere, cloud and rain is an important parameter for communication. In this paper, the measurement and assessment of these parameters will be discussed.

1. *Measurement of Atmospheric Attenuation*

To study the attenuation characteristics of the atmospheric window in microwave band, measurements will be presented. In the microwave band atmospheric scattering could be neglected. Therefore the atmosphere could be considered as a nonscattering medium.

(1) *Solar radiation method*

The solar and atmospheric radiation measurements are carried out by using microwave radiometers in Beijing. At different zenith angles, the antenna points to the sun and the neighbouring sky, then we can obtain atmospheric attenuation

$$\Gamma_o = -\frac{d}{dsec\theta}\ln(T_{as} - T_\varphi) \ , \tag{14}$$

where θ is zenith angle, T_{as} is antenna temperature in sun's direction, T_φ is a antenna temperature in background sky direction of the neighbour. In Sept.–Oct. 1983, at Peking University, Beijing, the measurements of atmospheric attenuation were conducted against calculations from radiosonde data, as shown in Fig.14. In 8.5 mm waveband, the average value of remote sensing is 0.066 and that of radiosonde calculation is o.o633. The atmospheric attenuation is larger when there exist clouds in the sky.

(2) *Remote sensing method*

In Sept.–Oct. 1981, at Peking University, Beijing, attempt was made to use measurements of multifrequency 5 mm—1.35 cm radiometers (frequency: 52.9, 54.5, 22.235, and 35.3 GHz) to derive the atmospheric temperature–humidity profile and atmospheric attenuation spectrum. The results are in agreement with radiosonde calculations. The atmospheric attenuation of 8 mm—1.35 cm waveband is found to depend on surface humidity.

2. *Prediction of Rain Attenuation*

For microwave communication engineering, the local rain characteristics and rain–attenuation probability should be understood. For the above purpose, the rainfall regularity and frequency 1—300 GHz rain attenuation probability in Beijing have been studied. The rainfall attenuation of surface–satellite link communication has been predicted.

Analysing rainfall materials of 1981–1987 in Beijing, we have gained the probability of rainfall in Beijing, which was compared with D_2, D_3, E zone distribution of Crane and K, L zone distribution of CCIR, showing that Beijing rainfall characteristics are similar to Crane D_3 and CCIR L distributions. The probability of rainfall attenuation has been studied for Beijing surface–satellite communication.

VII. MICROWAVE RADIOMETER COMBINED WITH RADAR FOR RAINFALL MEASUREMENT

The error in radar rain intensity measurements is mainly caused by instability of radar constant and the uncertainty of raindrop spectrum. From simulation tests, the error in rain intensity measured by radar is much larger. In the same condition, the error in rain measurements by dual–wavelength radar or radiometer–radar system is much smaller. But the radiometer–radar system is much simpler than the dual–wavelength radar. Therefore we took the method of radiometer–radar system for rain measurements.

Radar measurements of rainfall have good spatial resolution but not so good in accuracy, while radiometer measurements of rainfall have good accuracy in rain water content, but its spatial resolution not good. Radiometer–radar system has good results in both spatial resolution and accuracy of rain intensity. The rain emission, measured by radiometer, is used to correct the radar constant instability and the influence of raindrop spectrum uncertainty (see Du et al., 1984).

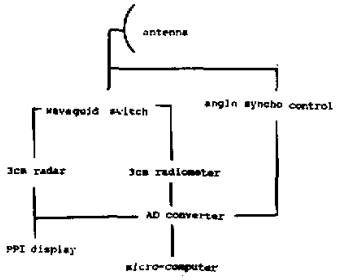

Fig.15. Radar–radiometer system ($\lambda = 3.2$ cm).

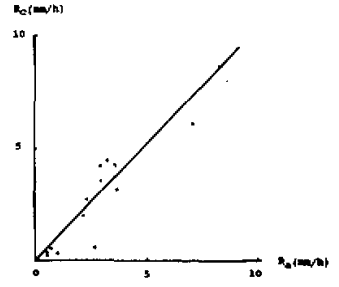

Fig.16. Rain intensity measurement with radar–radiometer system ($\lambda = 3.2$ cm) R_c vs rain intensity measurement with surface raingauge R_g, Jul. 27–28 1986, Beijing.

rain intensity (mm / h)	$(R_c - R_g)/R_g$(%)
0–1	36
1–3	26
3–6	20
6–10	9
average	25

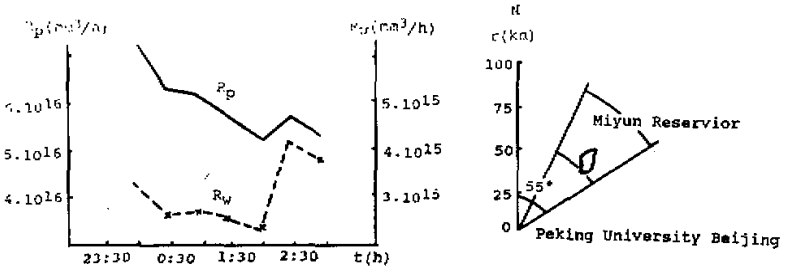

Fig.17. Variation of Area–rainfall measured with radar–radiometer system. R_p: rainfall of all observation area; R_w: rainfall of miyun Reservior area.

Some tests and principles of radiometer together with radar to detect rainfall have been studied in the Institute of Atmospheric Physics, Academia Sinica and a 3 cm and 8 mm radiometer system was used together with radar for observations of rain instensity (Lu and Lin, 1980).

The structure of the 3 cm radiometer–radar of Peking University is shown in Fig.15. The rain–intensity measured by radiometer–radar was compared with that measured by surface raingauge, as shown in Fig.16. The mean deviation between them is 25%. With microcomputer data processing, the area–rainfall in reservoir district can be obtained. The variation of area–rainfall of Minyun reservoir is shown in Fig.17. It would be helpful for hydrological prediction.

VIII. CONCLUDING REMARK

Microwave remote sensing of atmosphere, cloud and rain is a useful tool for nowcasting, weather modification and monitoring atmospheric environments. In China, tests to use the microwave remote sensing method for mesocale forecasting, and disaster prevention have been carried on. Some primary results obtained are interesting and encouraging.

REFERENCES

Blackadar A.K. (1979), High resolutuion models of the planetary boundary layer, *Advances in Environmental Science and Engineering*, **1**: 50–85.

Chahine M. (1970), Inverse problems in radiative transfer determination of atmospheric parameter, *J.Atmos. Sci.*, **27**: 960–967.

Delage Y. (1974), A numerical study of the nocturnal atmospheric boundary layer, *Quart. J. Roy. Met. Soc.*, **100**: 351–364.

Du Jinlin, Liu Baozhang and Zhao Bolin (1984), Study on rainfall measurement by means of combining radar with radiometer, *Acta Meteorologica Sinica*, **42**: 493–498.

Garrat J.R. and R.A.Brost (1981), Radiative cooling effects within and above the nocturnal boundary layer, *J. Atmos. Sci.*, **38**: 2730–2746.

Handbook of Remote Sensing Techniques, (1971), U.S.Dept. of Trade and Industry, TP 873–62, 145–173.

Hoggs D.C. *et al.* (1983), A steerable dual channel microwave radiometer for measurement of water vapor and liquid in the atmosphere, *J. Appl. Met.*, **22**: 789–806.

Huang Runheng et al. (1987), Remote sensing of total water vapor and liquid content of cloudy atmosphere by two wavelength microwave radiometry, *Scientia Atmospherica Sinica*, **11**: 397–403.

Lu Daren et al. (1980), Theoretical research of remote sensing of atmospheric cloud rain with radar–wave radiometer, Symposium on Meteorological Observation and Instrumentation of the Meteorological Society of China, 25–28.

Nimbus–5 User's Guides 1972.

Nimbus–6 User's Guides 1974.

Wei Chong at al. (1989), Microwave remote sensing of atmospheric water vapor and cloud liquid water over equatorial western Pacific Ocean with shipborne dual–wavelength radiometer, *Microwave Remote Sensing of Earth System*, A. Deepak Publishing, Hampton, 111–139.

Zhang Daling and R.A. Anthes (1982), A high resolution model of the planetary boundary larger–sensitivity test and comparison with SESAME–79 data, *J. Appl. Met.*, **21**: 1594–1609.

Zhao Bolin et al. (1981), The principle and test of microwave remote sensing, *Scientia Sinica*, **24**: 363–373.

Zhao Bolin et al. (1985), Atmospheric microwave radiation and remote sensing atmospheric water content, *Kexue Tongbao*(A Monthly J. Sciences), **30**: 85–89.

Zhao Bolin et al. (1985), A study on absorption characteristics of atmospheric window in microwave band, *Advances in Atmospheric Sciences*, **2**: 28–34.

Zhao Bolin et al. (1985), Experimental study on remote sensing on atmospheric sounding by means of multifrequency radiometers, *Scientia Sinica*, **28B**, 527–536.

Zhao Bolin (1987), Microwave radiometer and its application on remote sensing environments, *Atmospheric Radiation Progress and Prospects*, Sciences Press, Beijing, 282–290.

Zhao Bolin et al. (1987), A study of characteristics of atmospheric microwave absorption, *Acta Meteorologica Sinica*, **45**: 48–55.

Zhao Bolin et al. (1989), The simplification of 5 mm oxygen absorption coefficient formula, *Acta Meteorologica Sinica*, **47**: 103–112.

Zhao Bolin (1989), Study on microwave radiometer remote sensing of atmospheric sounding, oil slick and soil moisture, *Microwave Remote Sensing of Earth System*, A. Deepak Publishing, Hampton, 127–140.

Zhao Chonglong et al. (1983), 1.35 cm microwave radiometer for remote sensing of atmospheric humidity, *Scientia Sinica*, Ser.B, **26**: 759–768.

Zhou Xiuji, Lu Daren, Huang Runheng and Lin Hai (1982), *The Fundamental of Atmospheric Microwave Radiation and Microwave Radiation and Microwave Remote Sensing*, (in Chinese) Science Press, Beijing, 178pp.